International Research Journal of Multidisciplinary Scope (IRJMS), 2026;7(3):1003-1013

IRJMS

Original Article | ISSN (O): 2582-631X DOI: 10.47857/irjms.2026.v07i03.09489

Analysis of Ku to Ka Band Frequency Scaling for Tropical Country

Madhura Chakraborty*, Ranjana Ray, Sayanti Brahma

Department of Electronics and Communication Engineering, JIS College of Engineering, Kalyani, Nadia, West Bengal, India. *Corresponding Author's Email: madhura.chakraborty@jiscollge.ac.in

Abstract

In today's rapidly evolving world, maintaining uninterrupted communication services has become a major challenge. The expanding range of service-provider technologies, along with increasing variability in user demand has heightened the need to utilize higher-frequency communication bands. Frequencies above 10 GHz are especially appealing as they provide larger bandwidth, higher data rates, smaller device sizes and access to a broad spectrum. However, developing dependable wireless communication systems in these bands remains difficult, particularly in regions such as India. So for predicting rain attenuation in tropical countries, various methods are used and frequency scaling is one of them. In frequency scaling rain attenuation is predicted from one frequency to another frequency when data set of one band or frequency is completely unavailable. Few experiments are performed so far so for predicting rain attenuation for tropical and equatorial countries. In this work total 13 numbers of rain events are considered for Ahmedabad, for the year 2014 where frequency scaling is done on 20 GHz data to scale 30 GHz and later validation is done on measured signal. The result shows overestimation of scaled from measurement are present due to presence of attenuation, scintillation and DSD variation within the range of 0-5dB. But within the range of 5 dB to 30 dB the scaled and measured data matches quite well. After 30 dB due to measuring instrument's limitation, measured data is unavailable to validate with scaled data. So, in this work till 30 dB of attenuation, result is compared and model is developed and presented.

Keywords: DSD, Frequency Scaling, Ku Band, Rain Attenuation, Tropical Country.

Introduction

The remarkable improvement in world of internet along with the multimedia services enhanced the future plan for satellite communication. In satellite communications, use of popular C and Ku bands are already overused, so the band needs to move to higher frequency and that should be more than 10 GHz. For the reason, Ka-band (18-40 GHz) has achieved special concern due to the high demand. Ka-band satellite system has major drawback like increase in signal distortion caused by signal propagation impairment. Atmospheric attenuation in Ka-band is always very high, and things become serious issue in presence of rain. That's why Ka-band systems need newest technology to combat the impairment. Currently in India for commercial satellite communications, C and Ku-bands are commercially used. Ka band propagation studies are essential for accurate estimation of attenuation across pan India keeping in mind geographical and socio-economic variations to establish a proper links. This new generation of communication introduces a large number of innovative technologies. The statistical analysis of dynamic behaviour of signal attenuation helps to understand designing issues related to satellite communication for Ka band. Designed system is capable to increase power level to compensate the signal loss due to local climate conditions and helps in optimum use of available bandwidth. In this way a greater number of users can enjoy the benefit of reliable communication. Along with fade dynamics, scintillation that is abrupt fluctuation due to presence of cloud or rain or both is also very important study for SATCOM link design of Ka band. The associated parameters for link budget calculations are needed to be quantified for Ka band for suitably design of communication link. Prediction of rain attenuation from local rain data is a popular method. In addition, frequency scaling for rain attenuation is also an efficient technique. Therefore, investigation of frequency scaling for Ku to Ka band and in Ka band lower to higher range is also mention worthy for a suitable and proper FMT design. The Hodge model incorporates the maximum rainfall rate along the signal path, its spatial location on the propagation path, and the

(Received 02nd December 2025; Accepted 17th June 2026; Published 20th July 2026)

measured rain-cell length (1). It follows a Gaussian distribution for characterizing the positional occurrence of rainfall along the link. Another simple power-law model represents the ratio of frequencies and corresponding attenuation ratios, where the exponent varies for each frequency pair is observed (2). The Kheirallah model, derived from the ITU-R attenuation framework, assumes identical path reduction factors and path lengths for both frequencies (3). The Battesti model, designed for terrestrial microwave links, is developed from Canadian datasets and introduces a modified expression distinct from ITU-R, incorporating a new correction factor for scaled attenuation estimation (4). Limited studies have explored frequency scaling in tropical or equatorial regions. A study conducted in South Korea for 12.25 GHz, 19.8 GHz, and 20.73 GHz and signals were collected from Koreasat 6 and COMS 1. Scaled attenuation values at 19.8 GHz and 20.73 GHz exhibited higher errors in 0.001–1% probability range (5). Another study held in Malaysia explored scaling from 23 GHz to 38 GHz, with the Kheirallah model outperforming others, while power-law, Battesti, and Hodge models tended to overestimate measured attenuation (6). In another work in Singapore, frequency scaling between 15 GHz and 38.6 GHz over 10 months indicated that the scaling factor follows a square-foot dependency between 10 and 40 GHz (7). In a work ITU-R P.618-13 is compared (8). Recent work in Kolkata, India, using Ka-band data at 22.24 GHz, 26.24 GHz, and 31.4 GHz, found that ITU-R P.618-13 consistently overestimates attenuation above 10 dB when scaling was done for 31.4 GHz (9). One Study in Japan and Thailand scaled 12.59 GHz (Ku band) to 19.45 GHz (Ka band), using ITU-R methods to generate cumulative time percentages for various attenuation thresholds (10). In southern India, Ka-band measurements at 20.2 GHz and 30.5 GHz were used, and scaling from 20.2 GHz using ITU-Recommendation ITU-R 618.12 (11) allowed prediction at 30.5 GHz. In the work chi-square, error percentage, standard deviation, and RMS metrics were evaluated (12). A new India-specific method using real-time data scaled 20 GHz attenuation to 30 GHz is studied and the work introduced a model achieving approximately 95% accuracy at 2.5 dB (13). The method is based on the Simple Atmospheric Model (SAM) to compute the real-time spatial variability index of rain rate. One Delhi based study shows Ku to Ka band frequency scaling and result shows close matching with estimated and measured result (14). Many experiments were carried in another tropical country Nigeria for rain fade, slope and signal drop analysis (15-18). In Akure, an experiment was conducted for frequency scaling between year 2017 and 2018. The study shows the scaled attenuation at 16 GHz, 20 GHz, 30 GHz and 40 GHz respectively are 21.97 dB, 31.78 dB, 56.64 dB, 77.23 dB (19). The ITU-R has included few modifications on frequency scaling techniques and has recommended ITU-R 618.14 (20). The frequency scaling of satellite communication was experimentally introduced in a work where higher frequency attenuation data was unavailable (21, 22). SST was introduced in another work for prediction of rain attenuation in association with frequency scaling (23). A recent study at Shillong, hilly station of India with frequency scaling demonstrates Ku to Ka band rain attenuation estimation (24). A recent study on 5G communication for rain attenuation prediction was also conducted (25).

Methodology

Ka-band signals at 20.2 GHz and 30.5 GHz are recorded from GSAT-14, both in Ahmedabad and Delhi which provides an EIRP of 24 dBW. The satellite is having six numbers of Ku band along with six extended C band transponders for covering whole India. The satellite also carries two beacons in Ka and Ku band each for research purpose under satellite communication services.

In the site (both Ahmedabad and Delhi) the monsoon occurs from June to September, though rainfall also appears in May and occasionally in October. One 2.3m diameter parabolic dish antenna designed for horizontal and vertical polarization both and an identical data recording setup supplied by ISRO are employed for both beacons (20.2 GHz and 30.5 GHz). The signal is received with sampling rate of 1 Hz (both for 20.2 GHz and 30.5 GHz) and the rainfall rate (mm/hr) data is collected with 30 seconds temporal resolution. The 20.2 GHz receiver operates at 0° tilt with horizontal polarization, while the 30.5 GHz receiver uses 90° tilt with vertical polarization. Rainfall data is obtained from a tipping-bucket rain gauge that records rain intensity with a 1-min integration period. The gauge measures the time interval between two successive tips, and the instantaneous rainfall rate is derived as the ratio of rainfall per tip to the time between consecutive tips. 1-minute integration is then applied to generate the rainfall rate from the instantaneous measurements. A LPM is installed for monitoring environmental parameters in support for detailed analysis. The tipping-bucket rain gauge is kept in a open space having catchment area of 200 cm^2 and can measure 0.25ml amount of rain at tip. The time resolution is 1 tip per second and measures all the tipping times with the GPS receiver that is connected with the rain gauge.

Under an ISRO project at the Delhi Earth Station of the ISRO Centre (28°61'N latitude, 77°18'E longitude and 280 MSL), a 2.4-m diameter antenna with an elevation angle of 33.3° and an azimuth angle of 117.5° is used for the Ka-band, while a 4.6-m antenna with an elevation angle of 55° and an azimuth angle of 220.4° is deployed for Ku-band reception. Both receivers operate with a sampling interval of one second. Rainfall is recorded using a tipping-bucket gauge with 0.2-mm resolution as reported in a work (14). This work is used for all Ku to Ka based frequency scaling analysis in this work.

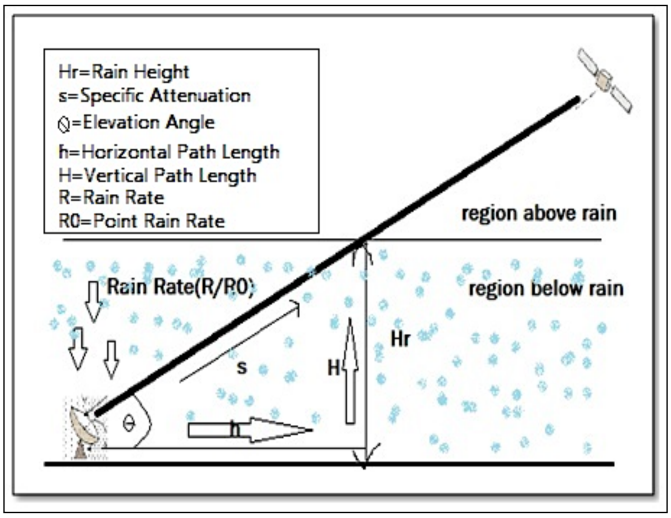

Figure 1: Signal Propagation through Troposphere and its Associated Parameters

Figure 1 illustrates the signal propagation process through the atmosphere and the associated parameters. The total attenuation A(f,t) in Equation [1] at frequency f and time t represents the time integral of specific attenuation during rainfall over the duration of signal travel along the propagation path.

$$A(f,t) = \int_0^{Lr} S(f, t, L, D, n(D)dL \qquad [1]$$

In the Equation [1], L is length of path in km and S is specific attenuation in dB/km and propagation path length during rain is L_r.

The specific attenuation at Equation [2] is dependent on frequency, time, path length, drop diameter and DSD mentioned as n(D) here.

$$S = aR^b \qquad [2]$$

Specific attenuation of a particular place is expressed as Equation [2] where a and b are frequency dependent power law co-efficient and R in point rain fall rate of a particular location in mm/hr

$$A(f,t)= \int_0^{Lr} S(f, R(t, L)dL \qquad [3]$$

So, the total attenuation in signal path can be derived as Equation [3]. For this estimation Equation [3], path length and rain rate values are needed. If local data is not available then ITU-R 837-5 is used for point rain fall rate prediction. Otherwise, SAM or Stutzman and Dishman can be used too. In this analysis 20.2 GHz and 30.5 GHz is mentioned as 20 GHz and 30 GHz in some places for enhancing readability.

The SAM model expresses the rain rate value as Equations [4, 5] with threshold value of rain rate as 10mm/hr,

$$R(t, h) = R_0(t) \qquad [4]$$

for R_0<10 mm/hr,

$$R(t,h) = R_0(t)\exp[-\gamma \ln\left[\frac{R_0}{10}\right] h] \quad [5]$$

for R_0>10 mm/hr,

In Equation [4, 5] the term h is rain height in Km and γ is the rain profile factor estimated from best fitting curve tool.

$$S(R_0,h) = aR_0{}^{b} \quad [6]$$

For R0<10 mm/hr,

$$S(R_0,h) = aR_0{}^{b}\exp[-\gamma b \ln\left[\frac{R_0}{10}\right] h] \quad [7]$$

For R0>10 mm/hr,

For rain rate less than 10mm/hr and more than that is presented in Equations [6, 7] separately. With the combination of Equations [2-5] following the slant path's' having length 'L' through rain presented separately in Equations [6, 7], the total attenuation could be predicted as Equation [8].

$$A = \int_0^L \alpha(s)ds = aR_0{}^{b}\int_0^L \exp\left[-\gamma b \ln\left[\frac{R_0}{10}\right] h\right] ds \quad [8]$$

Later the Equation [8] is modified with horizontal path length (h) to vertical path length (H) conversion and elevation angle is also taken care off for Equation [9] as below

$$A = aR_0{}^{b}\int_0^{Hr} \exp\left[-\frac{\gamma b \ln\left[\frac{R_0}{10}\right] H}{\tan\theta}\right] dH/\sin\theta \quad [9]$$

Integrating the H up to Hr the Equation [9] is modified in Equations [10-12] respectively

$$A = aR_0{}^{b}\left[1-\exp\{-\gamma b\cot\theta \ln[(\frac{R0}{10})Hr]\right]/[\gamma b\cos\theta \ln\left[\frac{R0}{10}\right] \quad [10]$$

$$A = (aR_0{}^{b})[1-\exp[-\gamma' bHr\mathrm{cosec}\theta]]/[\gamma' b] \quad [11]$$

Where,

$$\gamma' = \gamma \ln[\frac{R0}{10}]\cos\theta \quad [12]$$

Results and Discussion

For this analysis on frequency scaling, the measured attenuation data at 20 GHz and 30 GHz, along with the corresponding rainfall rate data for Ahmedabad for the entire year 2014, are utilized for both frequencies. In this study, the 20 GHz data are applied for scaling to 30 GHz, and the estimated values are subsequently validated using the measured 30 GHz signal for the same location. The analysis is performed for a total of 13 rain events recorded in Ahmedabad. One event on 14 July 2014 is illustrated in Figure 2, showing three continuous hours attenuation for both the frequencies.

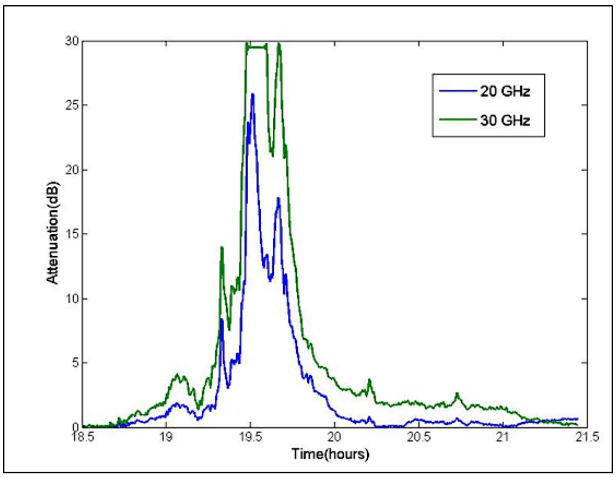

Figure 2: Plotting of Attenuation (both Frequency) From 18.50 pm to 21.50 pm

To determine the long-term cumulative distribution, the complete dataset of specific attenuation measured at both frequencies and the corresponding point rainfall rate for the same percentage of time is plotted together for the entire period of 2014. In establishing the relationship between specific attenuation and point rainfall rate, the frequency-dependent coefficients provided in ITU-R P.838 are used, and the rainfall rate $R_{0.01}$ is examined through a curve-fitting approach using MATLAB to obtain the power-law coefficients and finally the relation between specific attenuation to rainfall rate is established. For the year 2014, the values of 'a' and 'b' derived from the Equations are presented in Table 1.

Table 1: Power Law Coefficient for Finding Specific Attenuation for Ahmedabad

Frequency	'a' Coefficient Value	'b' Coefficient Value
20 GHz	0.9876	1.0943
30 GHz	0.2403	0.9485

So, for 20 GHz the Equation [13] becomes

$$A_{20} = 0.09876(R)^{1.0943} \quad [13]$$

Whereas the specific attenuation (dB/km) for 30 GHz Equation [14] is measured as

$$A_{30} = 0.2923(R)^{0.9676} \quad [14]$$

If the corresponding ITU-R P. 838-3 has been observed it has given the value of a and b as
(As signal is horizontally polarized) in the Equations [15, 16]

$$A_{20} = 0.09164(R)^{1.0568} \quad [15]$$

$$A_{30} = 0.2403(R)^{0.9485} \quad [16]$$

According to a study, the measured value of 'b' in both cases is greater than the corresponding ITU-R values of b at each frequency (14). This indicates that the rain DSD in Ahmedabad differs significantly from the data-set adopted in ITU-R P.838-3.

Now based on the measured relationship between point rainfall rate and specific attenuation that is Equations [13, 14], the frequency scaling Equation [17] are derived as below:

$$A_{30} = 1.6463(A_{20}) + 2.46 \quad [17]$$

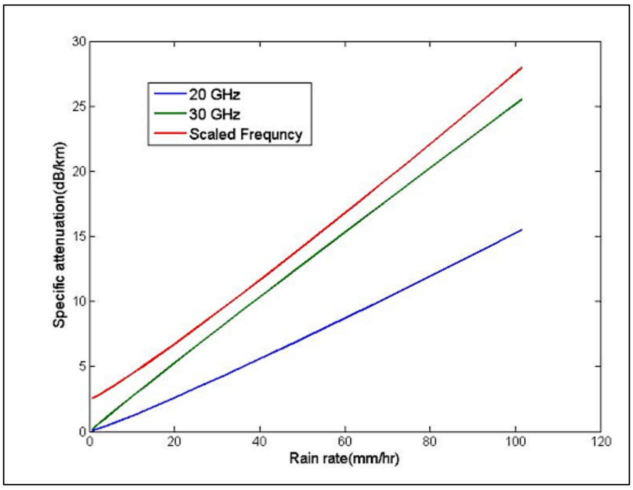

Figure 3: Relationship Between Specific Attenuation and Rainfall Rate with Measured and Scaled Specific Attenuation for the Whole Year of 2014, Ahmedabad

Now this Equation is used for comparing the measured data and finally Figure 3 is obtained. In Figure 3, Equation [17] is applied for frequency scaling using the 20 GHz signal attenuation. The results clearly shows that prediction for higher frequency is feasible through the scaling technique (14), though an overestimation relative to the measured values is evident across all point rainfall rate ranges in Ahmedabad during 2014. Subsequently, the same approach is applied to the measured attenuation in order to evaluate its overall usability on an event specific basis.

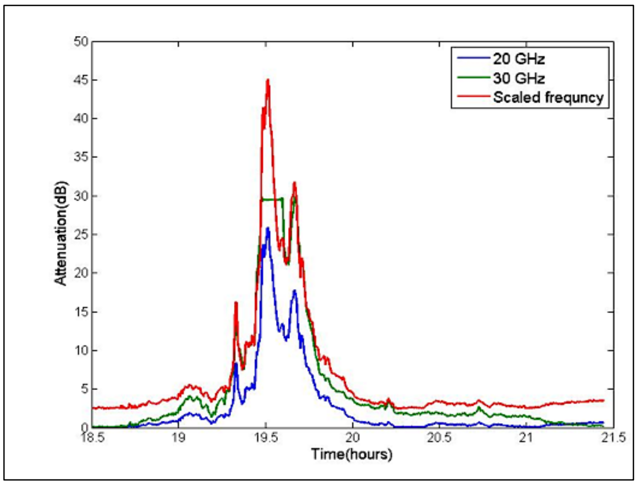

Figure 4: Scaled Frequency (Using 20 GHz) vs Measured Frequency for 30 GHz

In Figure 4, the scaled value corresponding to the 14th July, 2014 event and the measured 30 GHz attenuation are plotted together for comparison, along with the base frequency that is used for calculating the scaling results. There is a notably good agreement within the 5 dB to 30 dB range, and the outcome remains quite satisfactory on an event-wise basis when Equation [17] is applied. However, as indicated in Figure 4, within the 0 dB to 5 dB region, an overestimation of the scaled values relative to the measured data is observed. This may occur because, for attenuation values below 5 dB, both attenuation and scintillation effects coexist together with DSD-related variations that predominantly influence the lower attenuation levels. Since the 5 dB to 30 dB range is governed primarily by rain attenuation, the scaling-based prediction of 30 GHz attenuation becomes considerably reliable when Equation [17] is employed, as demonstrated in Figure 4, although values beyond 30 dB cannot be validated because of system constraints and the unavailability of measured 30 GHz data. Therefore, comparisons are restricted to attenuation levels up to 30 dB and the model is developed and presented accordingly.

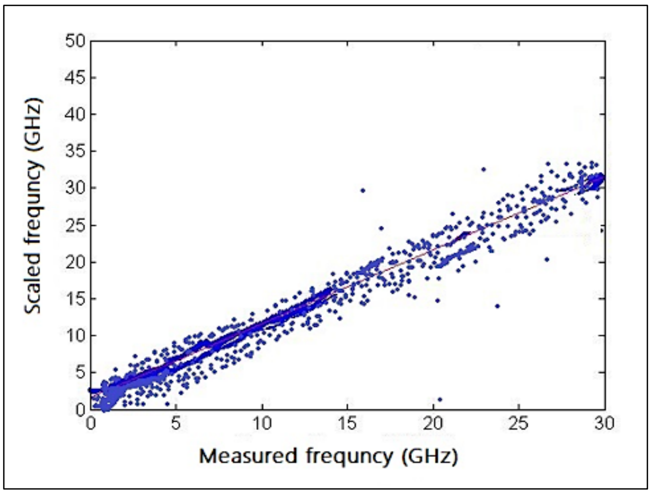

Figure 5: Scatter Plots to Show Estimation Accuracy

In Figure 5, the measured 30 GHz attenuation and the corresponding scaled values are plotted together to examine their behavior. Up to 30 dB, the accuracy remains high, and clear linearity appears between the measured and scaled results, demonstrating strong agreement and satisfactory performance.

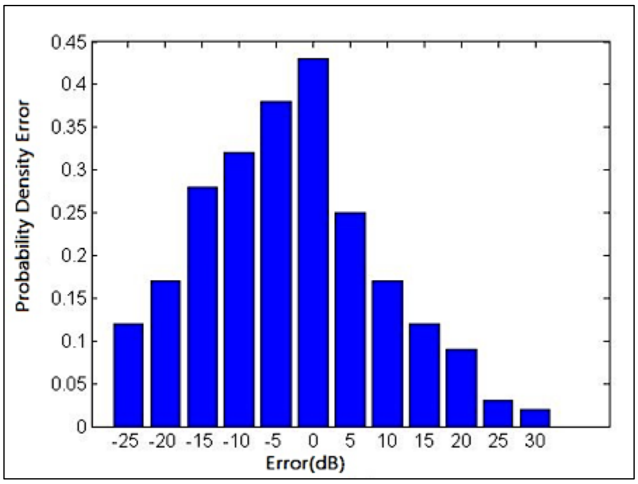

Figure 6: Plot of Probability Distribution of Errors

In Figure 6, the error, defined as the difference between the scaled (estimated) attenuation for 30 GHz derived from 20 GHz data and the measured attenuation at 30 GHz, is plotted to illustrate the probability distribution of the error. The distribution exhibits an almost normal behavior, with a noticeable spike near zero at a value of 0.42. To examine this characteristic further, a goodness-of-fit analysis is subsequently performed on the estimated dataset. The result shows an Equation [18] to best fit the error is

$$F(x) = a(\exp)^{bx} + c(\exp)^{dx} \qquad [18]$$

Where at 95% confidence bounds the value of coefficients are as follows: $a = 0.4892, b = 0.051, c = 0.4631$ and $d = -0.101$. Where $F(x)$ is function of error.

In this part of the work, the data utilized is derived from experimental observations reported in a study conducted in Delhi, India, a tropical country (14). The signal measurements supplied by ISRO are restricted to 20 GHz and 30 GHz, which have been employed for all analyses presented in the thesis so far. However, it is also necessary to examine the influence of frequency scaling on Ku-band signals for India and validate the results using the widely adopted model recommended in ITU-R 1623-13. Because the availability of Ku-band measurements is limited, the analysis considered here is based on 11.689 GHz from GSAT-8 and 20.199 GHz from the IPSTAR (Thaicomm-4) satellite, as described in the work (14).

According to the ITU-R P.618-13 recommendation, the frequency scaling approach is applicable for the 7–50 GHz range at a fixed geographic location. The recommendation states that when reliable measured attenuation data are available at a particular site, an empirical scaling relation can be applied to estimate the corresponding attenuation at other frequencies. This method predicts attenuation Equation [19] directly as a function of frequency and the latitude of the location, enabling accurate site-specific performance evaluation of Earth–space links.

$$A_2 = A_1 \left(\frac{\varphi_1}{\varphi_2}\right)^{1-H(\varphi_1,\varphi_2,A_1)} \qquad [19]$$

A_2 , A_1 both are excess rain attenuation uniformly probable values for the frequency of f_2 , f_1 (GHz) respectively in the Equation [19].

Here,

$$\varphi(f) = \frac{f^2}{1+10^{-4}f^2} \qquad [20]$$

$$H(\varphi_1, \varphi_2, A_1) = (1.12) \times 10^{-3} \left(\frac{\varphi_2}{\varphi_1}\right)^{0.5} (\varphi_1 A_1)^{0.55} \qquad [21]$$

According to the recommendation presented in Equations [20, 21], estimating rain attenuation using frequency yields more accurate results than estimations based on local rain rates.

The mentioned analysis is carried out using data reported in the past study (14). In this work, Ku-band rain attenuation was measured and plotted for different time exceedance levels, and similarly, Ka-band attenuation was also recorded and plotted. The experiment was conducted over two consecutive years beginning in 2012, with measurements collected primarily during the rainy season.

From the figures presented in the study, the Ku-band attenuation for various exceedance percentages starting from 0.01% is shown. At 0.01% exceedance, the measured attenuation at 11.69 GHz is approximately 12 dB. Likewise, for the Ka-band at 20 GHz, the rain fade for the same time exceedance is observed to be 24.6 dB. In Figure 7, the measured attenuation values at 11.69 GHz and 20 GHz are plotted together with the estimated Ka-band attenuation obtained using the ITU-R P.618-13 method. The computation is performed using Equations [19-21]. The results indicate that the ITU-R model consistently overestimates the measured attenuation. It is further noted that the deviation at lower exceedance percentages is greater than the deviation at higher exceedance levels. Specifically, an error of 11.69% is observed between the calculated and measured Ka-band attenuation.

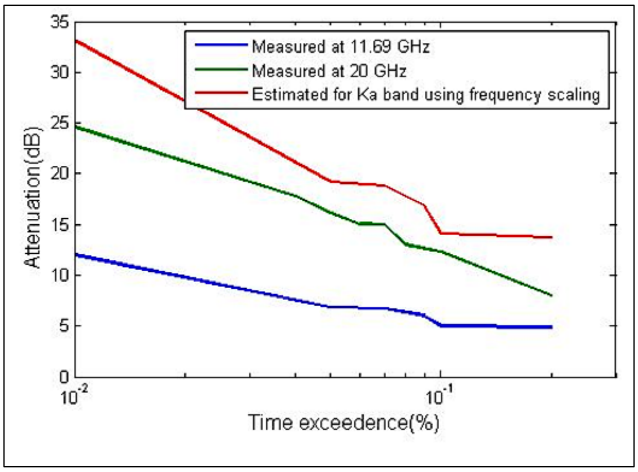

Figure 7: Comparative Study for Ku, Ka Band and Predicted Rain Attenuation (dB) Using Frequency Scaling (Delhi)

These findings clearly demonstrate that the ITU-R model and its associated coefficients are not sufficiently accurate for Ku-to-Ka band frequency scaling in rain attenuation prediction. This discrepancy may arise from regional variations in parameters such as rain, fog, mist, cloud structure, and differences in drop size distribution between temperate and tropical climates. Since the ITU-R model is predominantly based on temperate-region data, its performance deviates when same data set is applied to tropical environments. Therefore, the development of a new, locally optimized frequency scaling model is essential for accurate rain attenuation prediction in tropical regions.

Conclusion

This work focuses on frequency scaling for predicting rain attenuation when only one reliable measured attenuation dataset is available. This prediction approach is considered more effective than estimating attenuation directly from measured rain rate. The chapter begins with a discussion of the established frequency-scaling models reported till date, along with recent event-based scaling techniques. The study is divided into two major sections. The first section presents an approach for predicting frequency scaling from 20 GHz attenuation data to corresponding 30 GHz attenuation for Ahmedabad for the year 2014. In this case, since measured 30 GHz data are available, they are used for validating the scaled estimates. The analysis begins by obtaining the point rain rate for Ahmedabad and computing the corresponding specific attenuation from the measured 20 GHz signal by dividing the measured attenuation by the effective path length (Le) using the ITU-R P.618-13 formulation. The relationship between specific attenuation and point rain rate is then established as shown in Table 1. The same procedure is applied for 30 GHz for subsequent use. The rain-rate term in the specific attenuation expression for 30 GHz is then replaced, and a new set of coefficients is derived. Using the measured 20 GHz attenuation values, the scaled 30 GHz specific attenuation is obtained. Comparison of the scaled and measured 30 GHz attenuation indicates moderate overestimation. However, event-wise application of the same Equation yields good agreement for attenuation values between 5 dB and 30 dB, although the matching deteriorates below 5 dB due to scintillation effects and above 30 dB likely due to signal disruption or limited data availability due to instrumental limitation. When repeated for 13 rain events, strong linearity between measured and scaled attenuation is observed. The error probability distribution between scaled and measured values peaks at 0 dB, and a goodness-of-fit analysis is carried out on the estimated data. The resulting error Equation is presented with 95% confidence bounds.

The second part of the study examines Ku-to-Ka band frequency scaling for Delhi. Since the available dataset from ISRO for this research includes only Ka-band measurements, data from the published work, were used for Ku-band measurements. In this analysis, the Ku-band attenuation is treated as the reference, and scaled attenuation at 20.2 GHz is derived using the ITU-R frequency scaling method. The scaled attenuation is then compared with the measured Ka-band values, and significant overestimation is observed for Ku-to-Ka band scaling. This confirms that ITU-R-based frequency scaling is not suitable for tropical regions and highlights the need for appropriate model modification.

The work is done in both Ahmedabad and Delhi for Ka band and Ku band analysis of result. As the noise floor level of used instrument is fixed, few signals got redundant beyond the signal label of 30dB and more. Also, only monsoon dataset of 2014 was available for analysis both for 20 GHz and 30 GHz and for that the data point got restricted to only 13 events. If more data could be arranged in future more accurate estimation and validation could be possible to enhance the work to make it reliable to satellite communication providers. Hilly terrain data of Sikkim and Shillong is under consideration in future to complete the tropical dataset.

Abbreviations

DSD: Drop size distribution, EIRP: Effective Isotropic Radiated Power, ITU-R: International Telecommunication Union Recommendation, Ka: K above, Ku: K under.

Acknowledgment

The authors gratefully acknowledge the scientists at the Space Applications Center, ISRO, for providing the experimental data used in this study. Faculty Scheme and the ISRO–RESPOND programme are also sincerely acknowledged along with JIS College of Engineering and RFMO of JIS Group for providing laboratory facility.

Author Contributions

Madhura Chakraborty: Conceptualization, Methodology, Software, Investigation, Ranjana Ray: Visualization, Original Draft Preparation, Validation, Sayanti Brahma: Reviewing, Re-editing.

Conflict of Interest

There is no conflict of interest in this present research paper. This research work is not a part of any other studies and it is our original work.

Data Availability

The data used in this study were obtained from the Space Applications Centre (SAC), ISRO, and are not publicly available However; the data can be made available from the corresponding author upon reasonable request, subject to approval from the data provider.

Declaration of Artificial Intelligence (AI) Assistance

The author declares that Grammarly and QuillBot were used solely for language enhancement and text editing, particularly for grammar checking and improving structure (https://www.grammarly.com, https://www.quillbot.com) of the sentences. The authors take full responsibility for the content's originality, interpretation and accuracy.

Ethics Approval

Not applicable.

Funding

No direct financial support is received by authors. Therefore, the acknowledgment is included in the present article.

References

1. Hodge DB. Frequency scaling of rain attenuation. IEEE Trans Antennas Propag. 1977;25:446–447. doi:10.1109/TAP.1977.1141580
2. Drufuca G. Rain attenuation statistics for frequencies above 10 GHz from rain gauge observations. Journal de Recherches Atmosphériques. 1974;79(1–2):399–411. https://www.scirp.org/reference/referencespapers?referenceid=1443087
3. Kheirallah HN. Prediction techniques of rain and multipath outage statistics for line-of-sight radio communication systems [PhD thesis]. Ottawa, Canada: Carleton University; 1980. doi:10.22215/etd/1980-00547
4. Segal B. Rain attenuation statistics for terrestrial microwave links in Canada. Commun Res Cent Rep. 1982;1351-E. https://publications.gc.ca/site/eng/9.894574/publication.html
5. Shrestha S. Characterization of rain specific attenuation and frequency scaling method for satellite communication in South Korea. Int J Antennas Propag. 2017;2017:8694748. doi:10.1155/2017/8694748
6. Islam MR, Chebil J, Tharek AR. Frequency scaling of rain attenuation from 23- to 38-GHz microwave signals measured in Malaysia. Proc Asia-Pacific Microwave Conf. 1999. doi:10.1109/APMC.1999.833712
7. Zhou ZX, Li LW, Yeo TS, Leong MS. Cumulative distributions of rainfall rate and microwave attenuation in Singapore's tropical region. Radio Sci. 2000;35(3):751–756. doi:10.1029/1999RS900094
8. International Telecommunication Union. Propagation data and prediction methods required for the design of Earth-space telecommunication systems. ITU-R Recommend. 2016;618-13. https://itu-rpy.readthedocs.io/en/latest/validation/itur618_13.html#validation-results-itu-r-p-618-13
9. De A, Maitra A. Radiometric measurements of atmospheric attenuation over a tropical location. Radio Sci. 2020. https://doi.org/10.1029/2020RS007093
10. Chodkaveekityada P, Fukuchi H. Time diversity evaluation for attenuation mitigation using attenuation data in Thailand and Japan. Int J Satell Commun Netw. 2016;35(4):295–305. doi:10.1002/sat.1184
11. International Telecommunication Union. Propagation data and prediction methods required for the design of Earth-space telecommunication systems. ITU-R Recommend. 2015;618-12. https://www.itu.int/dms_pubrec/itu-r/rec/p/R-REC-P.618-12-201507-S!!PDF-E.pdf
12. Usha A, Karunakar G. Preliminary analysis of rain attenuation and frequency scaling method for satellite communication. Indian J Phys. 2020. doi:10.1007/s12648-020-01748-w
13. Acharya R. A simple real-time frequency scaling technique for rain attenuation and its performance. Int J Satell Commun Netw. 2020. doi:10.1002/sat.1337
14. Sujimol MR, Acharya R, Singh G, Gupta RK. Rain attenuation using Ka- and Ku-band frequency beacons at Delhi Earth Station. Indian Journal of Radio Space Phys. 2015;44:45–50 https://www.researchgate.net/publication/283096969_Rain_attenuation_using_Ka_and_Ku_band_frequency_beacons_at_Delhi_Earth_Station
15. Ogunsona DA, Ojo JS, Ashidi AG, Ajewole O. Characterization of rain fade dynamics for Ku-band satellite communication systems in a tropical location. J Phys Conf Ser. 2021;2034(1):012006. doi:10.1088/1742-6596/2034/1/012006
16. Ashidi AG, Ojo JS, Ajayi OJ. Evaluation of concurrent variation in rain specific attenuation and tropospheric amplitude scintillation over Akure, Southwest Nigeria. Earth Syst Environ. 2021;5:547–559. doi: 10.1007/s41748-021-00225-6
17. Igwe KC, Oyedum OD, Ojo JS, Obiyemi OO, Ibrahim AG. Computation of rain-induced attenuation at centimetric wave band for slant path communication in North Central Nigeria. Malays J Sci. 2024;43(3). doi: 10.22452/mjs.vol43no3.13
18. Lawal YB, Ojo JS, Falodun SE. Variability and trends in rain height retrieved from GPM and implications on rain-induced attenuation over Nigeria. Heliyon. 2021;7(10):e08108. doi: 10.1016/j.heliyon. 2021.e08108
19. Toriola WA, Ojo JS, Ashidi AG. Characterization of rain specific attenuation and frequency scaling technique for satellite communication systems in a tropical location. J Phys Conf Ser. 2021;2034(1): 012019. doi:10.1088/1742-6596/2034/1/012019
20. International Telecommunication Union. Propagation data and prediction methods required for the design of Earth-space telecommunication systems. ITU-R Recommend P.618-14.2021. https://itu-rpy.readthedocs.io/en/latest/apidoc/itu618.html
21. Laster JD, Stutzman WL. Frequency scaling of rain attenuation for satellite communication links. IEEE Trans Antennas Propag. 1996;44(10):1347–1353. doi: 10.1109/8.475986
22. Al-Saegh AM, Elwi TA, Abdullah OA, Sali A, Aljumaily AHJ. Rain attenuation frequency scaling for satellite communication systems. In: Proceedings of the 7th International Conference on Space Science and Communication (IconSpace); 2021:318–322. doi:10.1109/IconSpace53224.2021.9768738
23. Luini L, Panzeri A, Riva CG. Enhancement of the synthetic storm technique for the prediction of rain attenuation time series at EHF. IEEE Trans Antennas Propag. 2020;68(6):4825–4836. doi:10.1109/TAP.2020.2981682
24. Verma P, Chakraborty S, Chakraborty M. Frequency scaling of rain attenuation at Ka band over tropical

hill station, Shillong. Proc URSI Reg Conf Radio Sci. 2022. doi:10.23919/URSI-RCRS56822.2022.10118456

25. Zegerek BN. Evaluation of rain attenuation models for 5G frequencies: Regions in Turkey. J Brilliant Eng. 2024;2:4912. doi: 10.36937/ben.2024.4912

How to Cite: Chakraborty M, Ray R, Brahma S. Analysis of Ku to Ka Band Frequency Scaling for Tropical Country. Int Res J Multidiscip Scope. 2026;7(3):1003-1013. DOI: 10.47857/irjms. 2026.v07i03.09489